Identification of protein interactions of grapevine fanleaf virus RNA-dependent RNA polymerase during infection of *Nicotiana benthamiana* by affinity purification and tandem mass spectrometry

Larissa J. Osterbaan[1]†, Victoria Hoyle[1], Michelle Curtis[2], Stacy DeBlasio[3], Keith D. Rivera[4]‡, Michelle Heck[2,3] and Marc Fuchs[1,*]

Abstract

The RNA-dependent RNA polymerase ($1E^{Pol}$) is involved in replication of grapevine fanleaf virus (GFLV, *Nepovirus*, *Secoviridae*) and causes vein clearing symptoms in *Nicotiana benthamiana*. Information on protein $1E^{Pol}$ interaction with other viral and host proteins is scarce. To study protein $1E^{Pol}$ biology, three GFLV infectious clones, i.e. GHu (a symptomatic wild-type strain), GHu-$1E_{K802G}$ (an asymptomatic GHu mutant) and F13 (an asymptomatic wild-type strain), were engineered with protein $1E^{Pol}$ fused to a V5 epitope tag at the C-terminus. Following *Agrobacterium tumefaciens*-mediated delivery of GFLV clones in *N. benthamiana* and protein extraction at seven dpi, when optimal $1E^{Pol}$:V5 accumulation was detected, two viral and six plant putative interaction partners of V5-tagged protein $1E^{Pol}$ were identified for the three GFLV clones by affinity purification and tandem mass spectrometry. This study provides insights into the protein interactome of $1E^{Pol}$ during GFLV systemic infection in *N. benthamiana* and lays the foundation for validation work.

Grapevine fanleaf virus (GFLV) is a member of the genus *Nepovirus* in the family *Secoviridae* [1–4]. Its two positive-sense single-stranded genomic RNAs carry a genome-linked viral protein (VPg) at their 5′ end and are polyadenylated at their 3′ end [1, 3]. Expression of the two genomic RNAs is by monocistronic translation and proteolytic processing [1, 3]. GFLV RNA1 encodes five proteins for genome replication and polyprotein maturation, including protein 1A (46 kDa) of unknown function [3], a putative ATP-dependent helicase with membrane- and nucleoside triphosphate-binding motifs (protein $1B^{Hel}$, 88 kDa) [3, 5], a genomic-linked protein (protein $1C^{VPg}$, 3 kDa) [3, 5], a cysteine protease (protein $1D^{Pro}$, 24 kDa) [3, 6] and the RNA-dependent RNA polymerase (protein $1E^{Pol}$, 92 kDa) [3, 5, 7]. RNA2 encodes three pro-teins for RNA2 replication (protein $2A^{HP}$), movement (protein $2B^{MP}$) and encapsidation (protein $2C^{CP}$) [1, 3]. Systemic GFLV infection *in planta* requires both RNA1 and RNA2 [8].

Replication of GFLV occurs on endoplasmic reticulum-derived vesicles in infected plant cells and requires *de novo* lipid synthesis [3]. GFLV RNA1-encoded protein $1C^{VPg}$ and RNA2-encoded protein $2A^{HP}$ localize to the perinuclear replication compartments that contain double-stranded RNA molecules [3]. Little is known about the involvement of other viral proteins in replication although GFLV RNA1-encoded proteins $1E^{Pol}$ and $1B^{Hel}$ are suspected to be essential [3]. In addition, no information is available on the interaction of protein $1E^{Pol}$ with other GFLV proteins and host proteins for replication.
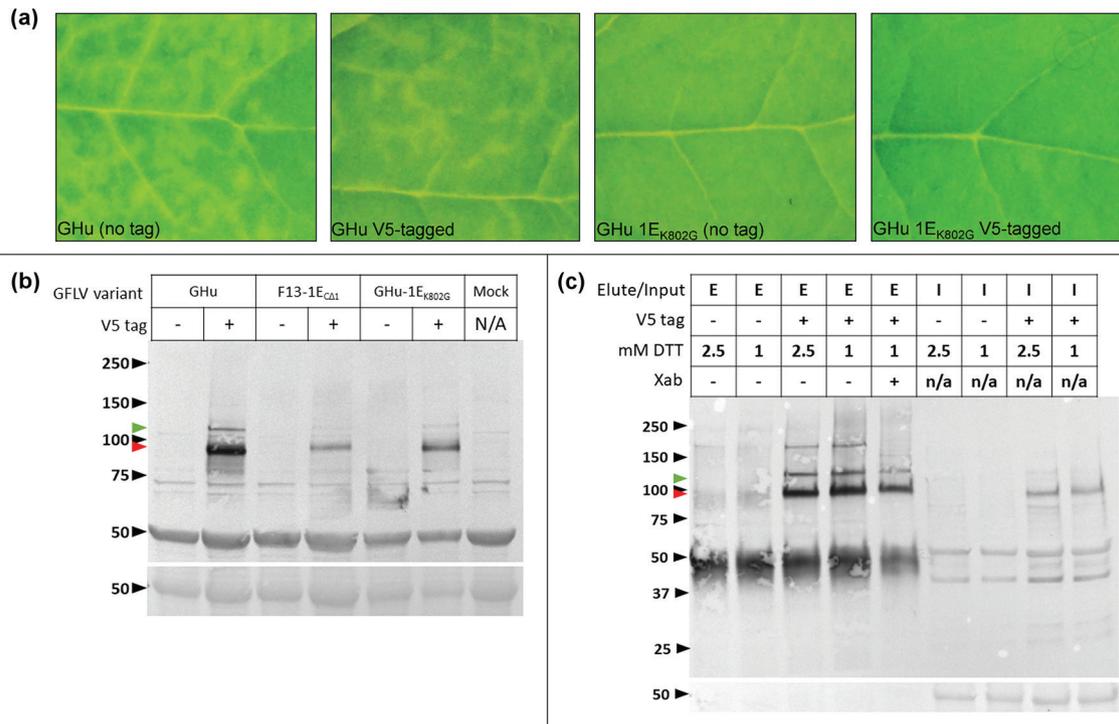
(a)

Fig. 1. (a) Symptom development in *Nicotiana benthamiana* plants infected with GFLV strain GHu or GHu-1E$_{K802G}$, an asymptomatic mutant of GFLV-GHu in which lysine 802 of protein 1E^{Pol} was mutated to glycine, and their corresponding version for which protein 1E was tagged with a V5 epitope. Insets show close-ups of vein clearing symptoms (first and second panels) and asymptomatic leaves (third and fourth panels) at six dpi. (b) Detection of protein 1E^{Pol}:V5 accumulation in *N. benthamiana* leaf tissue systemically infected with wild-type (-) or V5-tagged 1E^{Pol} (+) GFLV strains GHu and F13-1E$_{CΔ1}$, and mutant GHu-1E$_{K802G}$ by western blot with an anti-V5 antibody. TSP from a mock-inoculated *N. benthamiana* were used as a control. (c) Analysis of affinity purified 1E^{Pol} complexes in TSP from *N. benthamiana* leaves systemically infected with GFLV-GHu or GFLV-GHu-1E:V5 by western blot. TSP were extracted in lysis buffer 4 amended with 1X Halt protease inhibitor cocktail (Thermo Fisher Scientific) and further diluted 1:5 in DTT-free lysis buffer. Inputs were affinity purified with V5 polyclonal antibody (Invitrogen PA1-993) conjugated to Protein A Dynabeads (Invitrogen). The top row of lane labels indicates (e) elution products or (i) input fractions of the affinity purification. The second row indicates V5-tagged (+) or non-tagged (-) GFLV-GHu. The third row indicates the concentration of DTT included in the lysis buffer. The fourth row indicates whether the V5 polyclonal antibody used for affinity purification was untreated (-) or cross-absorbed against TSP from healthy *N. benthamiana* tissue (+). Proteins were probed with a polyclonal anti-V5 antibody (Invitrogen PA1-993, non-cross-absorbed) and a goat anti-rabbit alkaline phosphatase-conjugated secondary antibody (Invitrogen T2191) and developed with 1-Step NBT/BCIP solution. The predicted molecular weight of (i) V5-tagged 1E^{Pol} (93 kDa) is indicated with a red arrowhead, and (ii) a putative V5-tagged 1D^{Pro}E^{Pol} (117 kDa) or 1C^{VPg}1D^{Pro}E^{Pol} (120 kDa) precursor is indicated with a green arrowhead. Bottom panels show Ponceau staining of the RuBisCO large subunit. Molecular weight standards (kDa) are shown by black arrowheads.

Similarly, the molecular mechanisms underpinning GFLV symptom development remain largely unknown although recent advances have been made in model herbaceous hosts. For example, GFLV strain F13 produces a hypersensitive response triggered by the RNA2-encoded protein 2A^{HP} on inoculated leaves of *Nicotiana occidentalis* [9]. In contrast, GFLV-F13 produces an asymptomatic infection in *N. benthamiana,* while GFLV strain GHu produces distinct vein clearing symptoms on apical leaves of this plant species [7, 10]. A symptom determinant for vein clearing of GFLV-GHu was recently mapped to residue 802 of the RNA1-encoded protein 1E^{Pol}. This residue, which is a lysine in GFLV-GHu, is necessary but not sufficient for vein clearing development [10].

While much work has been done to describe molecular events of GFLV infection [3, 11], information about the molecular context of protein 1E^{Pol} during infection, in particular its protein interactants, is lacking. Here, we built on our previous work and developed a method to isolate protein 1E^{Pol} from protein extracts of *N. benthamiana* infected with GFLV and initiated a proof-of-concept study of the 1E^{Pol} protein interactome via affinity purification coupled to tandem mass spectrometry. To this end, tagging GFLV protein 1E^{Pol} was essential because, in our hands, efforts to generate an antibody that specifically detected 1E^{Pol} were unsuccessful. Indeed, an antibody raised against a synthetic peptide (HVPSKTSFM-KVPDELC) designed in a conserved N-terminus sequence failed to unambiguously detect an immunoreactive product of the expected size in total soluble protein extracts of GFLV-infected *N. benthamiana* via SDS-PAGE and western blot detection, although the same approach was successful in a
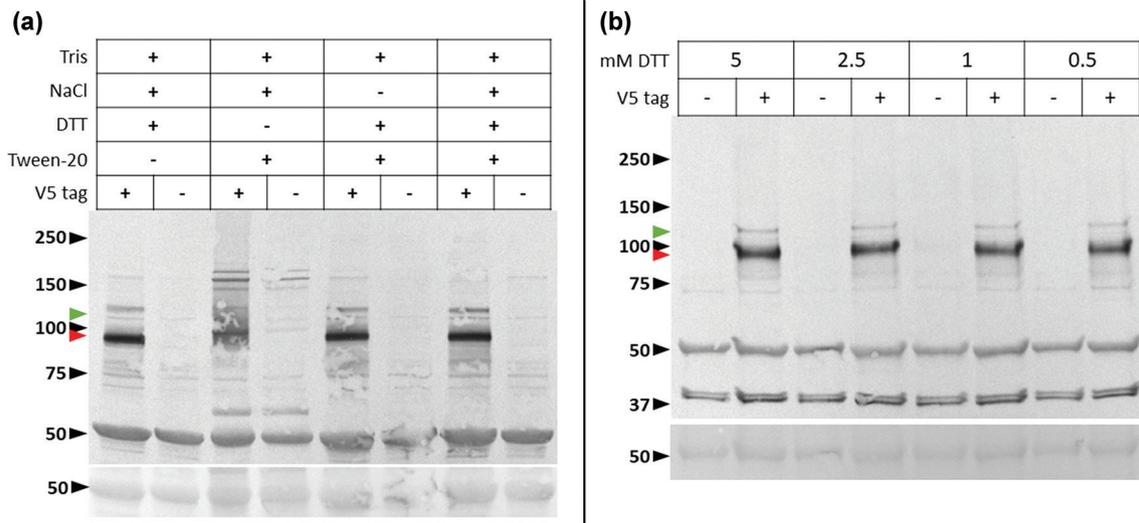
Fig. 2. Optimization of lysis buffer and extraction conditions of V5-tagged grapevine fanleaf virus (GFLV) protein $1E^{Pol}$ from systemically infected *Nicotiana benthamiana* tissue. (a) TSP extracted with lysis buffer one and lysis buffer one without (-) NaCl, DTT, or Tween-20. Single elimination of components from lysis buffer identified DTT as necessary for efficient detection of GFLV $1E^{Pol}$ from *N. benthamiana* tissue. (b) TSP extracted using lysis buffer 4 amended with 5.0 mM or 2.5 mM DTT, followed by a 1:5 post-extraction dilution with DTT-containing lysis buffer 4 (final DTT concentration of 5 and 2.5 mM, respectively) or DTT-free lysis buffer 4 (final DTT concentration of 1 and 0.5 mM, respectively). Top images show western blots of total soluble proteins (TSP) extracted from cryogenically milled *N. benthamiana* leaves systemically infected with either GFLV-GHu containing V5-tagged $1E^{Pol}$ (+) or wild-type GFLV-GHu $1E^{Pol}$ (non-tagged, -). Bottom images show Ponceau staining of the RuBisCO large subunit. Proteins were probed as described in Fig. 1. Molecular standards (in kDa) are shown by black arrowheads. The predicted molecular weight of V5-tagged $1E^{Pol}$ (93 kDa) is indicated with a red arrowhead, and that of a putative V5-tagged $1D^{Pro}E^{Pol}$ (117 kDa) or $1C^{VPg}1D^{Pro}E^{Pol}$ (120 kDa) precursor is indicated with a green arrowhead.

previous study [7]. Thus, we decided to tag protein $1E^{Pol}$ as an alternative to producing an antibody against $1E^{Pol}$.

The C-terminus of GFLV protein $1E^{Pol}$ was tagged by inserting the sequence of one of five common epitope tags, i.e. V5 [12], FLAG [13], 3XFLAG [14], HA [15] or myc [16] (Table S1, available with the online version of this article), in GFLV RNA1 cDNA constructs using the Q5 Site-Directed Mutagenesis Kit (New England Biolabs). Plasmids pCLEAN-F131-35S, pCLEAN-GHu1-35S and pCLEAN-GHu-1E$_{K802G}$-35S [10] served as PCR and cloning templates for tagging experiments using specific primers (Table S2). The GFLV RNA1 cDNA constructs are cloned within a cauliflower mosaic virus 35S expression cassette for expression *in planta* [10, 12]. Following *Agrobacterium tumefaciens*-mediated delivery of recombinant pCLEAN GFLV RNA1 constructs in the presence of pCLEAN-GHu-2–35S by syringe infiltration of *N. benthamiana* leaves [10, 17], only V5-tagged GFLV strains GHu and GHu-1E$_{K802G}$, an asymptomatic mutant of GHu for which the lysine in position 802 of protein $1E^{Pol}$ was substituted by a glycine [10], established systemic infection. None of the other GFLV-GHu recombinant clones were infectious *in planta* (Table S3). Typical vein clearing symptoms were observed in apical leaves for GFLV-GHu but no symptoms were apparent for GHu-1E$_{K802G}$ (Fig. 1a). These phenotypes were consistent with those of untagged viruses [7, 10, 17]. In addition, GFLV-GHu and its mutant were detected in uninoculated, apical *N. benthamiana* leaves by DAS-ELISA using GFLV specific antibodies (Bioreba 120642) and their $1E^{Pol}$:V5 protein (~93 kDa) accumulated in protein extracts from

apical leaves, as shown by SDS-PAGE and western blot detection with an anti-V5 antibody (Invitrogen PA1-993) (Fig. 1b, red arrowhead). In addition, an anti-V5 immunoreactive protein band of higher molecular mass (~117 kDa) was apparent in western blot for GFLV-GHu and GHu-1E$_{K802G}$ (Fig. 1b, green arrowhead). This protein was detected in the affinity purifications using cross-absorbed and non-cross-absorbed antibodies. It could correspond to the $1D^{Pro}E^{Pol}$ (117 kDa) or $1C^{VPg}1D^{Pro}1E^{Pol}$ (120 kDa) precursors (Fig. 1b, c).

For GFLV strain F13, a similar epitope tagging approach abolished infectivity *in planta*. Only mutants GFLV-F13-1E$_{CΔ1}$:V5 and GFLV-F13-1E$_{CΔ4}$:V5, in which a single or four residues were truncated at the C-terminus of protein $1E^{Pol}$ prior to the addition of the V5 epitope tag, established a systemic infection in *N. benthamiana*, as shown by DAS-ELISA using specific antibodies (Table S3). Infection of GFLV-F13-1E$_{CΔ1}$:V5 and GFLV-F13-1E$_{CΔ4}$:V5 was asymptomatic, consistent with the phenotype of the untagged virus [7, 10, 17]. Less $1E^{Pol}$:V5 accumulated in *N. benthamiana* infected with GFLV-F13-1E$_{CΔ1}$:V5 compared to GFLV-GHu:V5 and GFLV-GHu1E$_{K802G}$:V5 following infection (Fig. 1b). More work is needed to explain this differential accumulation of protein $1E^{Pol}$:V5 between GFLV strains GHu and F13. Of the two GFLV-F13 tagged mutants only F13-1E$_{CΔ1}$:V5 reliably showed an anti-V5 immunoreactive $1E^{Pol}$:V5 signal in protein extracts from apical *N. benthamiana* leaves tested by western blot detection (Table S3). Thus, this mutant was further used in a comparative proteomics analysis of tagged and untagged virus isolates.

Table 1. Potential protein interaction partners of grapevine fanleaf virus RNA1-encoded protein 1E^{Pol} identified using affinity purification coupled to tandem mass spectrometry

Accession number*	Protein Annotation†	Fold-change enrichment/Spectral counts‡	P-value§	Peptide Sequence||	Peptide identification Probability¶	Mascot ion Score#	Mascot identity threshold
AFM91094	GFLV_1B^{Hel}	∞ (26/0)	0.01723	K/NLLGEHILAEEEK/L	100	74.1	34.1
AFM91094	GFLV_1D^{Pro}	∞ (48/0)	0.02712	R/GVTYSSVIPSYSSSYVR/-	100	72.6	37.1
NP_619689	GFLV_1E^{Pol}	6.364 (716/4)	0.04665	K/LLDNVNTALVELYLHGDR/T	100	126.1	30.9
Niben101Scf03607g00009	Plastid transcriptionally active 14 SET domain protein	∞ (15/0)	0.00576	K/VIQALDIYQDR/I	100	49.3	35.7
Niben101Scf06128g00004	Splicing factor 3B subunit 1	∞ (19/0)	0.03184	R/LGETFNETAIPLR/Y	100	55.9	34.2
Niben101Scf01006g03016	Dynamin-related protein 5A	∞ (20/0)	0.04766	R/VEVNGAAVESLER/M	100	60.7	37.5
Niben101Scf01814g05011	WD40 domain-containing protein	2.8 (38/3)	0.02337	K/LDLSEILYQITSR/F	100	61	31.6
Niben101Scf04225g02007	Translation initiation factor IF-2	1.7 (30/5)	0.03922	K/VAASEAGGITQGIGAYK/V	100	72.8	34.5
Niben101Scf00593g01002	P-type ATPase (PMA1)	1.2 (59/14)	0.04770	K/LFSEATNFNELNQLAEEAK/R	100	93.5	37

*Sequence accession number from NCBI (for viral proteins) and Sol Genomics databases (for plant proteins).

†Protein annotations derived from NCBI for viral proteins and manual curation using BLAST for plant proteins.

‡Fold-change enrichment for proteins computed as Log$_2$ (spectral counts in tagged samples/spectral counts in untagged samples).

§P-values computed using a Student's *t*-test.

\|\|Sequence of the top-scoring peptide used to identify the protein.

¶Estimate of Scaffold peptide identification probability based on the quality of the MS/MS spectrum to peptide sequence match.

#The ion score for an MS/MS match in Mascot is based on the calculated probability, P, that the observed match between the experimental data and the database sequence is a random event. The reported score is −10Log(P). Ion scores that are higher than the Mascot identity threshold indicate high quality matches.

The Mascot peptide identity threshold is the ion score with expected significance threshold to be 0.05.

4

GFLV recombinants carrying protein 1E^{Pol} with the epitope tags FLAG, 3XFLAG, HA or myc repetitively failed to establish systemic infection in *N. benthamiana* (Table S3). Interestingly, of the five epitope tags tested, V5 has the lowest proportion of acidic residues. The V5 epitope (1.4 kDa) has 7% acidic residues in contrast to the FLAG, 3XFLAG, HA and myc tags, which have 63, 50, 40 and 22% acidic residues, respectively (Table S1). A low proportion of acidic residues is consistent with the residue composition of the C-terminal 53 amino acids of protein 1E^{Pol} of GFLV strains GHu (1.9% acidic residues) and F13 (3.7% acidic residues), suggesting the functionality of protein 1E^{Pol} may depend on the charge of its C-terminus. It is also possible that epitope tags, except V5, might have affected the stability of protein 1E^{Pol} or its capacity to be properly translated. More work is needed to address these issues.

A replicated time course experiment in *N. benthamiana* via mechanical inoculation with GFLV-GHu-1E^{Pol}:V5 showed optimal accumulation of immunoreactive 1E^{Pol}:V5 in TSP of apical leaves at 6–9 dpi by SDS-PAGE and western blotting with an anti-V5 antibody. This optimal period corresponds with noticeable GFLV-GHu vein clearing symptoms at 4–6 dpi (Fig. 1a) and symptoms fading at 9–10 dpi.

Of the four lysis buffers [18–21] (Table S4) tested for the extraction of 1E^{Pol}:V5 at seven dpi, a reducing agent such as DTT was necessary to confidently detect an immunoreactive peptide (Fig. 2a). It may be that a reducing environment is necessary to dissociate protein 1E^{Pol} from membranes, nucleic acids or other macromolecules. In support of this hypothesis, GFLV 1E^{Pol} likely associates with endoplasmic reticulum-derived membranes for replication [3, 11, 22], although it might not bind to membranes by itself when expressed ectopically in *N. benthamiana*, suggesting a probable dependence on another viral protein, likely protein 1B^{Hel}, to anchor to the replication complex, as previously discussed [3]. Similarly, the polymerase domain-containing precursor protein of tomato ringspot virus, another nepovirus, associates with endoplasmic reticulum-derived membranes [23].

Affinity purifications of the 1E^{Pol}:V5 protein complexes were performed on TSP extracted from *N. benthamiana* systemically infected with GFLV-GHu-1E:V5, GFLV-F13-1E$_{CΔ1}$:V5 or GFLV-GHu-1E$_{K802G}$:V5 collected at seven dpi. Untagged GFLV strains GHu and F13 were used as negative controls. Three biological replicates were performed for each virus treatment. Affinity purification conditions were as previously described [18] with the following modifications. The anti-V5 tag polyclonal antibody was bound to Dynabeads Protein A (Life Technologies, Invitrogen) at a concentration of 10 μg antibody per 1 mg of beads and 5 mg of beads in 5 ml of diluted plant cell lysate were used. For protein extraction, lysis buffer 4 (Table S4), a HEPES-based lysis buffer, was supplemented with 2.5 mM DTT, the lowest concentration of DTT required for sufficient extraction of 1E^{Pol}:V5, and lysates were further diluted 1:5 in lysis buffer without DTT (Fig. 2) to minimize loss of 1E^{Pol}-plant protein interactions and inhibition of bait capture by the V5 antibody, respectively. Washes

of beads were performed with DTT-free lysis buffer and the full bead volume was subjected to on-bead trypsin digestion, as described [18]. Additionally, to enrich for 1E^{Pol}:V5 and reduce background binding during affinity purifications, the anti-V5 antibody was cross-absorbed by sodium sulphate precipitation [24] with proteins from a blend of *N. benthamiana* tissue infected with untagged GFLV-GHu, F13 and GHu-1E$_{K802G}$ in equal proportions. The antibody fraction was recovered by overnight dialysis, as previously described [18]. Cross-absorption of the anti-V5 antibody resulted in the loss of some anti-V5 immunoreactive protein bands of higher molecular mass in western blot detection (Fig. 1c).

Sample cleaned for mass spectrometry was performed using OMIX C18 100 μl tips (Agilent, A57003100). After trypsin digestion, peptides were eluted from beads in 100 μl 0.1% formic acid. Protein complexes were analysed on an Orbitrap Fusion Lumos mass spectrometer (Thermo Scientific) equipped with a nano-ion spray source coupled to an EASY-nLC 1200 system (Thermo Scientific). The liquid chromatography system was configured with a self-pack PicoFrit 75 -μm analytical column with an 8 -μm emitter (New Objective, Woburn, MA) packed to 25 cm with ReproSil-Pur C18-AQ, 1.9 μm material (Dr. Maish HPLC, GmbH).

Thermo RAW files were converted to Mascot generic files (.mgf) using ProteoWizard [25]. The protein search database was generated from amino acid sequences corresponding to all coding gene sequences from version 1.01 of the *N. benthamiana* genome assembly downloaded from the Sol Genomics Network [26], amino acid sequences from nepoviruses including mutant and natural strains of GFLV, plus common mammalian affinity purification contaminant proteins downloaded from NCBI. The Mascot v. 2.5.1 software used to search the mgf files identified an average of 722 protein groups per replicate. Search parameters included one fixed modification (cysteine: carbamidomethyl), two variable modifications (deamidation of asparagine and glutamine and/or methionine oxidation), trypsin enzyme specificity, one missed cleavage, a peptide mass tolerance of ±20 ppm, fragment mass tolerances of ±0.5 Da, and ion charge=2+, 3+ or 4+.

Data were imported into Scaffold Q+4.80.4 (Proteome Software Inc., Portland, OR) for spectrum counting analysis. Peptide and protein false discovery rates were set at <1.0% using the Peptide Prophet algorithm [27] with delta-mass correction. Protein identifications were accepted if they contained at least two identified peptides. Protein probabilities were assigned by the Protein Prophet algorithm [27]. Proteins that contained similar peptides and could not be differentiated based on tandem mass spectrometry analysis alone were grouped to satisfy the principles of parsimony.

Spectral counts for proteins in the tagged (*n*=9 biological replicates, each from independent plants) and untagged (*n*=5 biological replicates, each from independent plants) samples were compared using a Student's *t*-test to identify proteins that may bind to protein 1E^{Pol}, but not in a GFLV strain specific manner, because no host proteins were found

to be enriched when each virus strain was tested individually. Log_2 fold-change enrichment (tagged/untagged) was calculated to determine enrichment in the experiments with the tagged $1E^{Pol}$.

Three RNA1-encoded GFLV proteins were significantly enriched in the affinity purification experiments: $1E^{Pol}$, $1B^{Hel}$ and $1D^{Pro}$ (Table 1). A single peptide spectral matching to protein $1E^{Pol}$ was detected at low levels in three of the five untagged replicates (Table 1), consistent with minimal levels of non-specific binding of $1E^{Pol}$ to the beads or the anti-V5 antibody used in the affinity purifications. In contrast, $1E^{Pol}$ was abundantly detected in the tagged replicates, as expected, and proteins $1B^{Hel}$ and $1D^{Pro}$ were only detected in experiments with tagged protein $1E^{Pol}$ (Table 1). A total of six plant proteins were identified to co-purify with GFLV protein $1E^{Pol}$ at low levels (Table 1). Among the six plant proteins, three proteins were specifically found in the tagged $1E^{Pol}$ samples: plastid transcriptionally active 14 Set domain protein (pTAC14), splicing factor 3B subunit one protein and dynamin-related protein 5A. The other three plant proteins, WD40 domain-containing protein, translation initiation factor IF-2 protein and P-type ATPase (PMA1), were detected in both the tagged and untagged samples but were found to be enriched (1.2 to 2.8 Log_2-fold) in the tagged samples with a *P*-value <0.05 (Table 1).

Three of the plant proteins identified in complex with $1E^{Pol}$ have been shown to play a role in plant or animal virus infection. For example, protein pTAC14 is localized in the chloroplast and regulates plastid gene expression [28]; several virus proteins have been shown to be involved in a plasma membrane and chloroplast signalling pathway to suppress salicylic acid-dependent plant defenses [29]. In rice, the splicing factor 3B subunit one protein regulates the expression of genes involved in cell death and resistance responses [30]. Splicing factor 3B subunit one has also been characterized to interact with animal viruses and plays a critical role in the replication of human immunodeficiency virus [31]. Dynamin-related protein 5A is critical for plant infection by soybean mosaic virus (SMV, genus *Potyvirus*, family *Potyviridae*) [32]. Dynamin-related protein 5A was identified in purifications of SMV virions using proteomics and knock-down of dynamin-related protein 5A in plants inhibited SMV infection in soybean [32]. Most of the plant proteins reported in this study were also described in the interactome of purified potato leafroll virus (genus *Polevirus*, family *Luteovidae*) virions during infection of *N. benthamiana* [18]. Additionally, recent evidence supports a role for PMA1 in the induction of an immune response manifested by cell death in *N. benthamiana*, as shown by silencing and overexpression assays [33].

Our proof-of-concept study based on affinity purifications of V5-tagged $1E^{Pol}$ coupled with protein identification by tandem mass spectrometry provided a snapshot of the putative protein interaction network of protein $1E^{Pol}$ during systemic GFLV infection of *N. benthamiana*. Methods to optimize the extraction of protein $1E^{Pol}$ from plant tissue may increase the depth of proteomic coverage and lead to a more thorough characterization of the plant-virus interactome. GFLV protein $1D^{Pro}$, the viral protease which processes *in cis* and *in trans* the two viral polyproteins into individual mature peptides [1, 3, 5, 6, 11], was enriched in affinity purifications with V5-tagged $1E^{Pol}$, suggesting that $1D^{Pro}$ complexes with $1E^{Pol}$ during virus infection. The $1B^{Hel}$ helicase protein [1, 3, 5, 11] was also enriched as a protein interacting in complex with $1E^{Pol}$ during virus infection. It is also possible that protein $1D^{Pro}$ peptides are enriched in affinity purifications with $1E^{Pol}$ due to the presence of putative $1D^{Pro}1E^{Pol}$ or $1C^{VPg}1D^{Pro}1E^{Pol}$ precursors of polyprotein processing that were suggested by western blot analyses (Figs 1 and 2). More research is needed to test whether interactions between GFLV proteins $1E^{Pol}$, $1D^{Pro}$ and $1B^{Hel}$ are direct or indirect, to understand the stoichiometry of binding and the significance of these interactions during virus infection, in particular in replication.

Orthologous of most plant host proteins enriched in our data set were previously documented to be involved in virus-host interactions with other plant or animal viruses [18, 28–32]. These host protein candidates will need to be validated in follow-up genetic approaches to verify whether they have a role in GFLV infection in *N. benthamiana*.

References
1. Andret-Link P, Laporte C, Valat L, Ritzenthaler C, Demangeat G, *et al*. Grapevine fanleaf virus: Still a major threat to the grapevine industry. J Plant Pathol 2004;86:183–195.
2. Karasev AV, Dasgupta I, Fuchs M, Iwanami T. *Secoviridae*. 2019.
3. Schmitt-Keichinger C, Hemmer C, Berthold F, Ritzenthaler C. Molecular, Cellular, and Structural Biology of Grapevine fanleaf virus. Grapevine VirusesMolecular, cellular, and structural biology of grapevine fanleaf virus. Grapevine Viruses. Springer: Molecular Biology, Diagnostics and Management; 2017, pp. 83–107.
4. Thompson JR, Dasgupta I, Fuchs M, Iwanami T, Karasev AV, *et al*. ICTV virus taxonomy profile: Secoviridae. *J Gen Virol* 2017;98:529–531.
5. Ritzenthaler C, Viry M, Pinck M, Margis R, Fuchs M, *et al*. Complete nucleotide sequence and genetic organization of grapevine Fanleaf nepovirus rna1. *J Gen Virol* 1991;72:2357–2365.
6. Margis R, Viry M, Pinck M, Pinck L. Cloning and in vitro characterization of the grapevine fanleaf virus proteinase cistron. *Virology* 1991;185:779–787.
7. Vigne E, Gottula J, Schmitt-Keichinger C, Komar V, Ackerer L, *et al*. A strain-specific segment of the RNA-dependent RNA polymerase of grapevine fanleaf virus determines symptoms in *Nicotiana* species. *J Gen Virol* 2013;94:2803–2813.
8. Viry M, Serghini MA, Hans F, Ritzenthaler C, Pinck M, *et al*. Biologically active transcripts from cloned cDNA of genomic grapevine fanleaf nepovirus RNAs. J Gen Virol 1993;74:169–174.

9. Martin IR, Vigne E, Berthold F, Komar V, Lemaire O, *et al*. The 50 distal amino acids of the 2AHP homing protein of Grapevine fanleaf virus elicit a hypersensitive reaction on Nicotiana occidentalis. Mol Plant Pathol 2018;19:731–743.

10. Osterbaan LJ, Choi J, Kenney J, Flasco M, Vigne E, *et al*. The identity of a single residue of the RNA-dependent RNA polymerase of grapevine fanleaf virus modulates vein clearing in *Nicotiana benthamiana*. *Mol Plant Microbe Interact* 2019;32:790–801.

11. Fuchs M, Schmitt-Keichinger C, Sanfaçon H. A renaissance in nepovirus research provides new insights into their molecular interface with hosts and vectors. *Adv Virus Res* 2017;97:61–105.

12. Southern JA, Young DF, Heaney F, Baumgartner WK, Randall RE. Identification of an epitope on the P and V proteins of simian virus 5 that distinguishes between two isolates with different biological characteristics. *Journal of General Virology* 1991;72:1551–1557.

13. Hopp TP, Prickett KS, Price VL, Libby RT, March CJ, *et al*. A short polypeptide marker sequence useful for recombinant protein identification and purification. *Nat Biotechnol* 1988;6:1204–1210.

14. Hopp TP, Gallis B, Prickett KS. Metal-binding properties of a calcium-dependent monoclonal antibody. *Mol Immunol* 1996;33:601–688.

15. Schembri L, Dalibart R, Tomasello F, Legembre P, Ichas F, *et al*. The HA tag is cleaved and loses immunoreactivity during apoptosis. *Nat Methods* 2007;4:107–108.

16. Zeng Q, Si X, Horstmann H, Xu Y, Hong W, *et al*. prenylation-dependent association of protein-tyrosine phosphatases PRL-1, -2, and -3 with the plasma membrane and the early endosome. *J Biol Chem* 2000;275:21444–21452.

17. Osterbaan LJ, Schmitt-Keichinger C, Vigne E, Fuchs M. Optimal systemic grapevine fanleaf virus infection in Nicotiana benthamiana following agroinoculation. *J Virol Methods* 2018;257:16–21.

18. DeBlasio SL, Johnson R, Mahoney J, Karasev A, Gray SM, *et al*. Insights into the polerovirus–plant interactome revealed by coimmunoprecipitation and mass spectrometry. *Mol Plant Microbe Interact* 2015;28:467–481.

19. Nölke G, Cobanov P, Uhde-Holzem K, Reustle G, Fischer R, *et al*. Grapevine fanleaf virus (GFLV)-specific antibodies confer GFLV and Arabis mosaic virus (ArMV) resistance in *Nicotiana benthamiana*. *Mol Plant Pathol* 2009;10:41–49.

20. Jovel J, Walker M, Sanfaçon H. Recovery of *Nicotiana benthamiana* plants from a necrotic response induced by a nepovirus is associated with RNA silencing but not with reduced virus titer. *J Virol* 2007;81:12285–12297.

21. Dufresne PJ, Thivierge K, Cotton S, Beauchemin C, Ide C, *et al*. Heat shock 70 protein interaction with Turnip mosaic virus RNA-dependent RNA polymerase within virus-induced membrane vesicles. *Virology* 2008;374:217–227.

22. Ritzenthaler C, Laporte C, Gaire F, Dunoyer P, Schmitt C, *et al*. Grapevine fanleaf virus replication occurs on endoplasmic reticulum-derived membranes. *J Virol* 2002;76:8808–8819.

23. Chisholm J, Zhang G, Wang A, Sanfaçon H. Peripheral association of a polyprotein precursor form of the RNA-dependent RNA polymerase of Tomato ringspot virus with the membrane-bound viral replication complex. *Virology* 2007;368:133–144.

24. Clark M, Lister R, Bar-Joseph M. ELISA techniques. Weisbach A and Weisbach H (eds). In: *Methods for Plant Molecular Biology*. Cambridge, MA, USA: New York: Academic Press; 1988. pp. 742–766.

25. Kessner D, Chambers M, Burke R, Agus D, Mallick P. ProteoWizard: open source software for rapid proteomics tools development. *Bioinformatics* 2008;24:2534–2536.

26. Bombarely A, Rosli HG, Vrebalov J, Moffett P, Mueller LA, *et al*. A draft genome sequence of *Nicotiana benthamiana* to enhance molecular plant-microbe biology research. *Mol Plant Microbe Interact* 2012;25:1523–1530.

27. Ma K, Vitek O, Nesvizhskii AI. A statistical model-building perspective to identification of MS/MS spectra with Peptideprophet. *BMC Bioinformatics* 2012;13.

28. Gao ZP, Q-B Y, Zhao TT, Ma Q, Chen GX, *et al*. A functional component of the transcriptionally active chromosome complex, Arabidopsis pTAC14, interacts with pTAC12/HEMERA and regulates plastid gene expression. Plant Physiology 2011;157:1733–1745.

29. Medina-Puche L, Tan H, Dogra V, Wu M, Rosas-Diaz T, *et al*. A novel pathway linking plasma membrane and chloroplasts is co-opted by pathogens to suppress salicylic acid-dependent defences. *Cell* 2020;182:1109–1124.

30. Chen X, Hao L, Pan J, Zheng X, Jiang G, *et al*. Spl5, a cell death and defense-related gene, encodes a putative splicing factor 3b subunit 3 (sf3b3) in rice. *Mol Breeding* 2011;30:939–949.

31. Kyei GB, Meng S, Ramani R, Niu A, Lagisetti C, *et al*. Splicing factor 3B subunit 1 interacts with HIV Tat and plays a role in viral transcription and reactivation from latency. *mBio* 2018;9.

32. Wu G, Cui X, Chen H, Renaud JB, Yu K, *et al*. Dynamin-like proteins of endocytosis in plants are coopted by potyviruses to enhance virus infection. *Journal of Virology* 2018;92:23.

33. Choi D, Lee HY, Seo YE, Lee JH, Lee SE, *et al*. Plant NLR targets P-type ATPase for executing plasma membrane depolarization leading to calcium influx and cell death. bioRxiv 2020.